Accurate Measurement of Dynamic ON-state Resistance of GaN Devices under Reverse and Forward Conduction in High Frequency Power Converter

Li, K., Videt, A., Idir, N., Evans, P. & Johnson, M.

Accurate Measurement of Dynamic ON-State Resistances of GaN Devices Under Reverse and Forward Conduction in High Frequency Power Converter

Ke Li , *Member, IEEE*, Arnaud Videt , *Member, IEEE*, Nadir Idir , *Member, IEEE*, Paul Leonard Evans , and Christopher Mark Johnson , *Member, IEEE*

Abstract—Because of trapped charges in GaN transistor structure, device dynamic ON-state resistance R_{DSon} is increased when it is operated in high frequency switched power converters, in which device is possibly operated by zero voltage switching (ZVS) to reduce its turn-ON switching losses. When GaN transistor finishes ZVS during one switching period, device has been operated under both reverse and forward conduction. Therefore its dynamic R_{DSon} under both conduction modes needs to be carefully measured to understand device power losses. For this reason, a measurement circuit with simple structure and fast dynamic response is proposed to characterize device reverse and forward R_{DSon}. In order to improve measurement sensitivity when device switches at high frequency, a trapezoidal current mode is proposed to measure device R_{DSon} under almost constant current, which resolves measurement sensitivity issues caused by unavoidable measurement circuit parasitic inductance and measurement probes deskew in conventional device characterization method by triangle current mode. Proposed measurement circuit and measurement method is then validated by first characterizing a SiC-MOSFET with constant R_{DSon}. Then, the comparison on GaN-HEMT dynamic R_{DSon} measurement results demonstrates the improved accuracy of proposed trapezoidal current mode over conventional triangle current mode when device switches at 1 MHz.

Index Terms—Dynamic ON-state resistance, forward conduction, GaN transistor, high switching frequency, reverse conduction, soft switching.

I. INTRODUCTION

BECAUSE of low power losses and fast switching transition, integrating gallium nitride (GaN) power semiconductor devices into high frequency (HF) electrical energy conversion systems is becoming a hot research topic [1]–[4] to increase power converter power density. To design HF power converters, device power losses estimation becomes very important, as it determines whole system cooling equipment size, which is a key factor to influence on system power density. However, unlike silicon (Si) or silicon carbide (SiC) devices, GaN device has an unwanted characteristic, which is caused by the trapped charge in device buffer layer when device is in OFF-state. Those trapped charges will reduce device current conduction capability, resulting in increased ON-state resistance (R_{DSon}) compared with device theoretical value. It is to be noted that GaN device dynamic R_{DSon} values are normally not given in device datasheet, which makes its conduction power losses unpredictable in application. Furthermore, power semiconductor devices R_{DSon} is an important parameter for power electronics systems diagnosis, which can be used as an indicator to study the degradation of both device [5] and packaging [6]. Therefore, a clear understanding of GaN device dynamic R_{DSon} is also important for the study of power electronics systems health management. For those reasons, it is necessary to propose new characterization method to accurately measure GaN device dynamic R_{DSon} in HF power converters.

Even though GaN device fabrication process has been improved by different techniques, such as field-plate structure [7] and ameliorated device buffer layer [8], [9] to decrease dynamic R_{DSon} value, it is still found in reported research work [10]–[17] that commercial device dynamic R_{DSon} can increase to maximal 5–10 times bigger than device static R_{DSon} value depending on device operation conditions.

GaN device dynamic R_{DSon} measurement method reported in the above research work can be summarized into Table I, where there are in general indirect and direct measurement method. In indirect measurement method [10], whole system power losses is measured at first, then with knowledge of other losses present in the active and passive components, the device conduction losses can be indirectly obtained. However, the application of this method in device hard switching operation has not been

TABLE I
COMPARISON BETWEEN THE STATE-OF-THE-ART RESEARCH WORK AND PROPOSED METHOD IN THIS ARTICLE TO MEASURE GaN DEVICE DYNAMIC R_{DSon}

| Research work	Method	Switching mode	Current mode & device conduction	Not discussed
Galapon et al. [10]	Indirect	Soft switching	Quasi sinusoidal, forward & reverse	Sensitivity, hard switching
Badawi et al. [11], Cai et al., [12] Yang et al. [13], Foulkes et al., [14] Li et al. [15]	Direct	Hard switching	Quasi constant, forward	Soft switching, reverse current
Lu et al. [16], Li et al. [17]	Direct	Hard & Soft switching	Triangular, forward	Sensitivity, reverse current
This work	Direct	Hard & Soft switching	Trapezoidal, forward & reverse	-
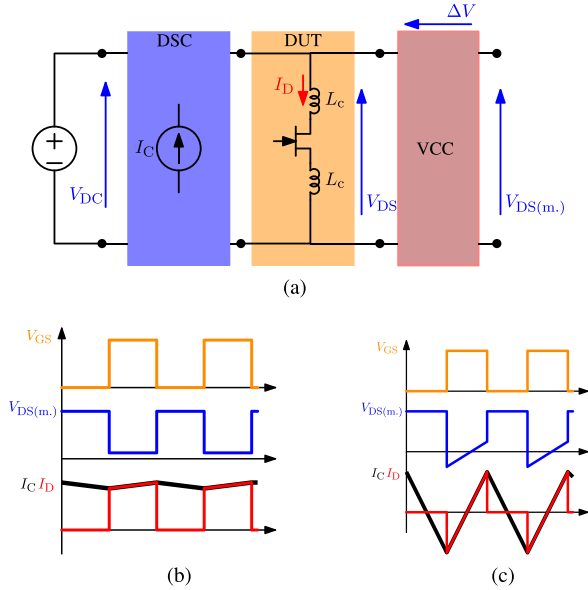
Fig. 1. Measurement circuit to measure GaN device dynamic R_{DSon} value. (a) Measurement circuit. (b) DUT hard switching. (c) DUT soft switching via TCM.

discussed, as device hard switching losses might cause measurement sensitivity issue, which needs to be further investigated.

In direct measurement method, GaN device conduction current and voltage are measured to obtain R_{DSon}. As illustrated in Fig. 1(a), measurement circuit is normally constituted by device switching circuit (DSC), device under test (DUT), and voltage clamping circuit (VCC). The main purpose of DSC (including current source I_C) is to control DUT OFF-state, ON-state time, and switching conditions. The aim of VCC is to alter the voltage across DUT V_{DS} to the measured voltage $V_{DS(m.)}$ by $V_{DS(m.)} = V_{DS} - \Delta V$, where ΔV is the voltage across VCC. ΔV should equal to V_{DS} when DUT is in OFF-state, while ΔV should be almost zero when DUT is in ON-state for measurement accuracy. Therefore, instead of measuring full range V_{DS} voltage, smaller $V_{DS(m.)}$ voltage is measured to improve the measurement resolution of the oscilloscope (with 8–12-b resolution). It can be also noted that parasitic inductance L_c from DUT branch is appeared in both DSC and VCC part, which is their common L_c when DUT is in operation.

In the published work [11]–[15], authors use different types of the circuit to investigate GaN device dynamic R_{DSon} value under hard switching condition, in which DUT gate source voltage V_{GS}, $V_{DS(m.)}$, and drain current I_D waveform are shown in

Fig. 1(b) (supposing I_C is in continuous mode). When DUT is in ON-state, it is always under forward conduction by a quasi-constant I_D, therefore L_c has little influence on dynamic R_{DSon} measurement results. However, because device can only operate at hard switching in the presented measurement circuits, the above research work cannot be directly applied to investigate GaN device dynamic R_{DSon} value in soft switching condition, where DUT is under reverse conduction.

To extend the method to the case when GaN device is operated in soft switching condition, authors in [16] and [17] have proposed a resonant tank in DSC and have controlled DUT in zero voltage switching (ZVS) via triangle current mode (TCM), in which its V_{GS}, $V_{DS(m.)}$ and I_D waveform are shown in Fig. 1(c). However, GaN device dynamic R_{DSon} is only measured under forward conduction in the above work. Additionally, measurement sensitivity issue due to voltage drop V_{L_c} by I_D fast transition di/dt has not been discussed.

It is important to measure GaN device dynamic R_{DSon} when device is under reverse conduction for the following reasons.

1) Soft switching is an effective method to reduce GaN device switching losses, so device can operate in HF to improve power converter power density. It is necessary to know the dynamic R_{DSon} value immediately after device leaves the OFF-state and begins conduction, but in soft switching operation, the device may be in a reverse conduction mode at this time. Only obtaining its dynamic R_{DSon} value under forward conduction may underestimate its conduction losses.

2) During deadtime between two transistors in a phase-leg, current flows reversely through one transistor after turn-OFF of the other. Therefore, it is important to understand this deadtime loss in HF power converters when using GaN devices [18], which requires VCC with reverse current blocking capability and low ΔV under DUT reverse conduction.

Therefore, the main objective of the article is to accurately measure GaN device dynamic R_{DSon} under both reverse and forward conduction when device operates at HF converter. The main contributions are as follows:

1) to propose a new VCC accordingly;
2) to study measurement accuracy and cause of the errors;
3) measurement sensitivity issues are resolved by new trapezoidal current mode (TZCM), where device is still operated at soft switching in HF and it brings practical benefits by adding delay between two phase-legs.

As shown in Table II, the presented results in this article extends device characterization area in terms of switching

TABLE II
COMPARISON BETWEEN OUR PREVIOUS PAPER [15] AND THIS ARTICLE

|	Previous paper	This paper
Converter operation frequency	<10kHz, transient-state to 0.1s	until 1MHz, steady-state>100s
Purpose	Dynamic R_{DSon} characterisation & modelling	Accurate dynamic R_{DSon} characterisation
Paper structure	Characterisation circuit & modelling method	Characterisation circuit & characterisation method
Measurement time	>1μs	>10ns
Operation conditions	hard switching, forward conduction	hard & soft switching, forward & reverse conduction
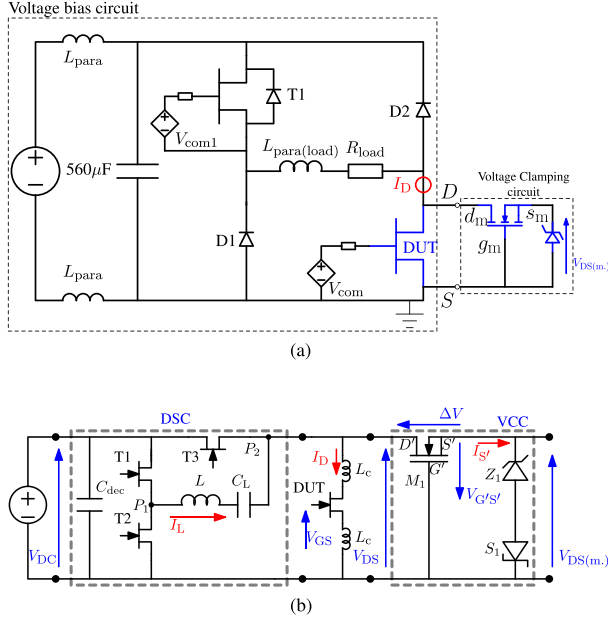
Fig. 2. Comparison of the electrical circuit between our previous work and this work to measure GaN device dynamic R_{DSon}. (a) Measurement circuit of our previous work in [15] to measure GaN device dynamic R_{DSon} only under forward conduction. (b) Measurement circuit of this paper to measure GaN device dynamic R_{DSon} under reverse and forward conduction.

Fig. 3. VCC static characteristics. (a) Two diodes unit characteristics. (b) M1 and two diodes unit characteristics.

frequency, measurement time, and device operation conditions than our previous work presented in [15]. It is an overall achievement by using new measurement circuit and TZCM measurement method.

This article is structured with following sections. In Section II, new measurement circuit is proposed to characterize GaN device dynamic R_{DSon} value in both reverse and forward conduction. In Section III, influence of measurement circuit L_c and other parameters (measurement probes deskew and oscilloscope offset voltage) on GaN device dynamic R_{DSon} measurement sensitivity is studied and TZCM is proposed. In Section IV, experimental measurement results are presented to validate proposed measurement circuit and method. This article is concluded in Section V.

II. MEASUREMENT CIRCUIT OF GaN DEVICE DYNAMIC R_{DSon} UNDER REVERSE AND FORWARD CONDUCTION

A. Measurement Circuit

In our previously used electrical circuit shown in Fig. 2(a) [15], DUT can only operate in hard switching condition under forward conduction. In order to extend DUT operation

conditions, another electrical circuit shown in Fig. 2(b) is proposed in this article, where GaN device dynamic R_{DSon} value under both reverse and forward conduction can be characterized. In this circuit, the DSC part is a standard H-bridge circuit with two phases including decoupling capacitor C_{dec}, three identical power semiconductor devices T1, T2, T3. By connecting an output inductor L and capacitor C_L between nodes P_1 and P_2, DUT can operate at soft switching by alternating inductor current I_L direction. VCC part is constituted by three main components—a depletion-mode MOSFET M_1 with threshold voltage (V_{th}) inferior to zero, a Zener diode Z_1, and a Schottky diode S_1. The measured voltage $V_{\mathrm{DS(m.)}}$ is between cathode (K) of Z_1 and cathode of S_1, which also equals to the reverse gate voltage $V_{\mathrm{G'S'}}$ of M1 ($V_{\mathrm{G'S'}} = -V_{\mathrm{DS(m.)}}$). Following components are chosen in the VCC part: M1 (BSP135, 600 V/100 mA, $V_{\mathrm{th}} \approx -1.6$ V), Z1 (BZT52C3V3, Zener voltage is 3.3 V), and S1 (RB751SM-40FH, 40 V/30 mA). The choice of those components is justified by the circuit analysis below.

The relation of current and voltage of each diode Z1 and S1 together with their unit characteristics under their connection is shown in $V_{\mathrm{G'S'}} - I_{\mathrm{S'}}$ plot in Fig. 3(a). It is to be noted that for the chosen components, M1 gate leakage current can be neglected in comparison with two diodes unit leakage current. Two diodes

unit static characteristic is then represented in the form of a surface in Fig. 3(b).

Static characteristics of M1 is also represented in Fig. 3(b) in the form of a surface, where M1 ohmic region and saturation region are illustrated. ΔV equals to $V_{D'S'}$ voltage, which defines the measurement error when DUT is in ON-state.

It can be observed that there is an intersection line between two surfaces, which represents common static characteristics of M1 and two diodes unit. Depending on DUT operation conditions, static characteristics of VCC follows this intersection line.

1) DUT OFF-state: Static characteristics of VCC is in intersection line AB. It is shown that $V_{G'S'}$ voltage is around M1 V_{th}, so M1 is in OFF-state and it withstands almost the whole dc voltage ($\Delta V \approx V_{\text{dc}}$). Measured $V_{DS(m.)}$ is around M1 opposite Vth value. In this condition, as shown in the projection of line AB in $I_{S'} - V_{D'S'}$ plane, leakage current of the chosen components in the VCC part is about 200 μA, which will not cause components self-heating.

2) DUT forward conduction: Static characteristics of VCC part is in intersection line ac. As long as DUT forward ON-state voltage $V_{DSon(F.)}$ is inferior to M1 opposite Vth, M1 operates in the ohmic region. As shown in the projection of line ac in $V_{G'S'} - V_{D'S'}$ plane, ΔV is much smaller than measured voltage $V_{DS(m.)}$ ($\Delta V = 10\ m$V when $V_{DS(m.)} = 1$V). Therefore, $V_{DS(m.)}$ equals to DUT forward ON-state voltage $V_{DSon(F.)}$.

3) DUT reverse conduction: $V_{G'S'}$ voltage is positive in this condition, so M1 operates at ohmic region (ON-state resistance less than 50 Ω). As reverse $I_{S'}$ is very small [less than 0.1 μA, see Fig. 3(a)], ΔV is less than 5 μV. Therefore, similar as DUT forward conduction, measured voltage $V_{DS(m.)}$ equals to DUT reverse ON-state voltage $V_{DSon(R.)}$.

Regarding the measurement accuracy, it can be noted that the proposed VCC is robust on drift of any temperature-dependent device static characteristics and it does not require any calibration of chosen devices, which is the case for using diode-type VCC in the literature [17]. Furthermore, it has reverse current blocking capability, which guarantees a wide operation range when DUT is under reverse conduction and during deadtime.

In terms of dynamic characteristics, proposed VCC improves the circuit dynamic response and M1 gate voltage overshoot, which is major drawback of transistor-type VCC analyzed by Gelagaev *et al.* in [19].

1) DUT OFF–ON transition: As $V_{G'S'}$ is around M1 V_{th} value when DUT is in OFF-state, M1 gate source capacitance $C_{G'S'}$ only needs a little charge (less than 0.1 nC) to increase $V_{G'S'}$ voltage superior to Vth during DUT ZVS transition. When $V_{G'S'}$ is superior to Vth, M1 output capacitance stored charge $Q_{oss'}$ (about 2 nC when DUT switches at 200 V) is dissipated in M1 channel quickly. Therefore, dynamic response of the VCC is fast to follow DUT OFF–ON transition. $Q_{oss'}$ of M1 is inferior to 20% of that of chosen DUT, which makes proposed VCC nonintrusive during measurement. Minimum $V_{DS(m.)}$ is determined by whether DUT body diode conducts during deadtime, which is normally a voltage drop of 2–3 V.

2) DUT ON–OFF transition: Maximum $V_{DS(m.)}$ is determined by $V_{G'S'}$ overshoot voltage during transition, where it is clamped by the chosen Z1 (3.3 V). As S1 has very small
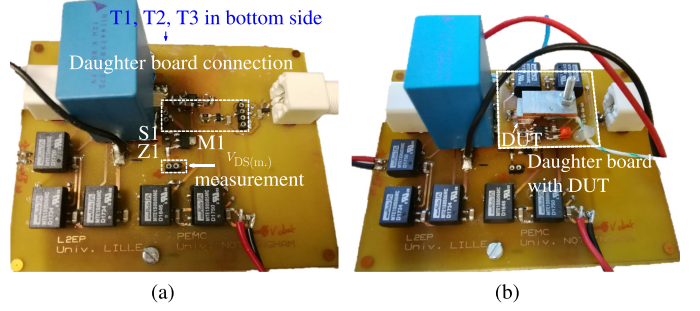

Fig. 4. Measurement circuit realization. (a) Mother board. (b) Mother board+Daughter board.
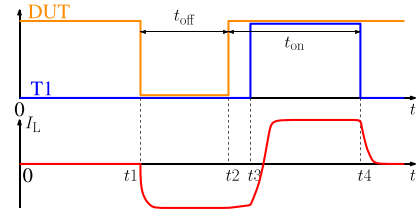

Fig. 5. Single-pulse control signal to measure power transistor reverse and forward ON-state resistance.

ON-state voltage drop, total overshoot voltage is inferior to 4 V during DUT transition, which improves M1 gate voltage surge immunity.

It can be concluded that in all the above DUT operation conditions, measured $V_{DS(m.)}$ equals to the $V_{G'S'}$ variation, which is from a few negative volts (bigger than -3 V) to a few positive volts (less than 4 V). Therefore, a small voltage division (500 mV/div or 1 V/div) of the oscilloscope can be used in the measurement to have an improved resolution on V_{DSon} value compared with a direct measurement (with 50 or 100 V/div).

Measurement circuit is realized with the photo shown in Fig. 4, where it is constituted by a mother board including same GaN-HEMT T1, T2, T3 (GS66502B, 650 V/7.5 A) with their gate drivers, alongside M1, Z1, S1 of VCC part and a daughter board including DUT with its gate driver. The advantage of this design is that only daughter board needs to be changed to characterize different types of DUT.

Validation of the circuit when device is operated at hard switching has been presented in [15]. Therefore, in this article, measurement results are focused on device soft switching operation.

B. Measurement Circuit Validation

By replacing LC_L by a RL branch between P_1 and P_2 at first in Fig. 2(b), a SiC-MOSFET (C2M0160120D, 1200 V/19 A, Vth = 2.6 V) with static R_{DSon} around 200 mΩ is characterized first by the above measurement circuit with single-pulse control signals of T1 and DUT given in Fig. 5. T2 and T3 are complimentary control signals of T1 and DUT, respectively.

From $0 - t_1$ [ee Fig. 6(a)], both DUT and T2 are in ON-state, therefore $I_L = 0$. Afterward, both T3 and T2 are in ON-state from $t_1 - t_2$ [see Fig. 6(b)], where I_L is charged in reverse conduction until steady state. DUT OFF-state time t_{off} is defined by this interval. Following that, both DUT and T2 are in ON-state from $t_2 - t_3$ [see Fig. 6(c)], where DUT is turned on at ZVS at t_2 and
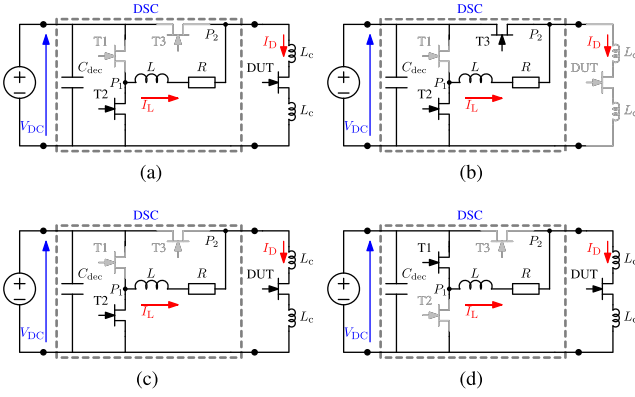
Fig. 6. Different circuit operation stages under given single-pulse control signal. (a) From $0 - t_1$. (b) From $t_1 - t_2$. (c) From $t_2 - t_3$. (d) From $t_3 - t_4$.

it begins conducting reversely I_L (I_L decreases toward zero with time constant $\frac{L}{R}$). At final step $t_3 - t_4$ [see Fig. 6(d)], both DUT and T1 are in ON-state, where I_L alternates direction until steady state in forward conduction (time constant is still determined by $\frac{L}{R}$). Thus, DUT ON-state time t_{on} is defined by $t_2 - t_4$ interval. A detailed analysis on DUT ZVS process has been presented by authors in [20]. Under this control sequence, DUT R_{DSon} under reverse and forward conduction ($R_{DSon(R.)}$ and $R_{DSon(F.)}$) can be obtained at $t_2 - t_3$ interval and $t_3 - t_4$ interval, respectively, under constant I_L. $R_{DSon(R.)}$ can be obtained under long t_{on} by choosing a big L and $R_{DSon(F.)}$ can be obtained quickly after I_L transition by using a small L. Therefore, by setting $t_2 - t_3$ stage length accordingly, both $R_{DSon(R.)}$ and $R_{DSon(F.)}$ can be obtained under similar t_{on} scale to compare.

As SiC-MOSFET does not suffer any dynamic resistance variation as GaN transistor, its obtained reverse and forward ON-state resistance by the proposed circuit can be used as a reference to verify proposed circuit dynamic response and accuracy. Measurement condition is: $V_{dc} = 200$ V and stabilized DUT ON-state current is 2 A. I_L is obtained in experiment measurement, and $I_L = I_D$ when DUT V_{GS} reaches ON-state gate voltage.

For the characterized SiC-MOSFET, as shown in Fig. 7(a) when DUT is in OFF-state, obtained $V_{DS(m.)}$ is clamped to reverse V_{th} of chosen depletion MOSFET ($Vth \approx -1.6$ V), which confirms the above circuit analysis and when it is under reverse conduction, DUT reverse ON-state voltage $V_{DSon(R.)}$ and current I_D can be measured quickly after $V_{GS} = 16$ V, which confirms the fast response of the presented measurement circuit. As shown in Fig. 7(b), when it is under forward conduction, DUT forward ON-state voltage $V_{DSon(F.)}$ and current I_D are measured when I_L is stabilized.

DUT $R_{DSon(R.)}$ and $R_{DSon(F.)}$ are then compared in Fig. 7(c) to show its variation with ON-state time t_{on}. Obtained DUT average reverse ON-state resistance ($\overline{R_{DSon(R.)}}$) by the proposed measurement method is about 161 mΩ, even with some noise on the measurement data, $R_{DSon(R.)}$ standard derivation ($\sigma_{R_{DSon(R.)}}$) is about 2.5 mΩ, which is only 1.6% to $\overline{R_{DSon(R.)}}$. In terms of DUT average forward ON-state resistance ($\overline{R_{DSon(F.)}}$), obtained value is about 174 with 2 mΩ on $\sigma_{R_{DSon(F.)}}$ (1.1% to $\overline{R_{DSon(F.)}}$). Those small relative $\sigma_{R_{DSon(R.)}}$ and $\sigma_{R_{DSon(F.)}}$ values prove the measurement consistency of the proposed circuit.

$\overline{R_{DSon(R.)}}$ and $\overline{R_{DSon(F.)}}$ between proposed method is then compared in Table III with their values obtained in device
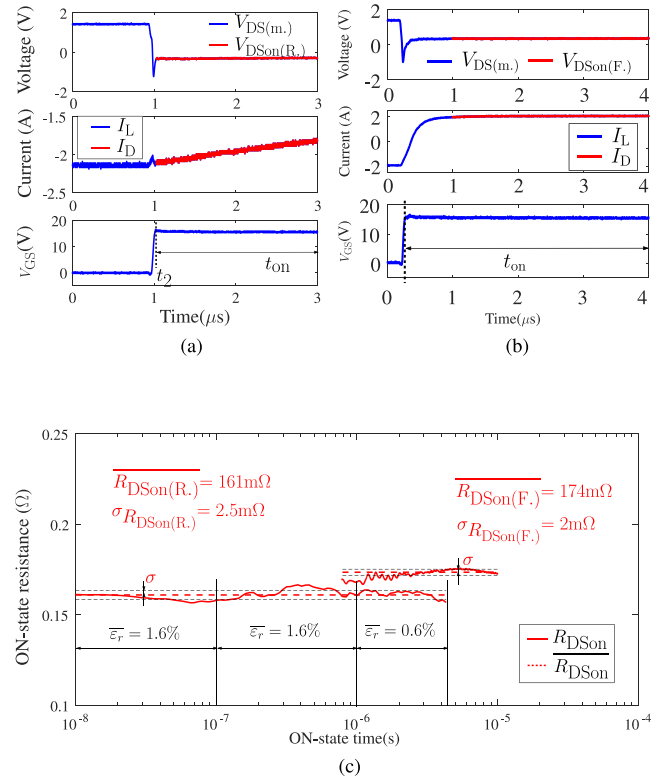
Fig. 7. SiC-MOSFET reverse and forward ON-state resistance measurement results. (a) Voltage and current waveform when SiC-MOSFET is reverse conduction. (b) Voltage and current waveform when SiC-MOSFET is forward conduction. (c) SiC-MOSFET reverse and forward ON-state resistance.

TABLE III
COMPARISON OF SiC-MOSFET $\overline{R_{DSon(R.)}}$ AND $\overline{R_{DSon(F.)}}$ BETWEEN PROPOSED METHOD AND DEVICE CURVE TRACER

	$\overline{R_{DSon(R.)}}$	$\overline{R_{DSon(F.)}}$
Proposed method	161 mΩ	174mΩ
Device curve tracer	163 mΩ	169 mΩ
Relative measurement error	1.2%	2.9%

curve tracer (B1505 A). Relative measurement error between the proposed method to the curve tracer is inferior to 2.9%, which confirms the measurement accuracy of the proposed circuit. It is to be noted that for SiC-MOSFET, obtained device $\overline{R_{DSon(R.)}}$ is slightly smaller than $\overline{R_{DSon(F.)}}$. This difference is supposed to be the SiC-MOSFET body diode conduction when DUT is under reverse conduction, which lowers DUT reverse $R_{DSon(R.)}$.

Response time of VCC is an important parameter to judge if it can be used to measure DUT dynamic R_{DSon} when DUT is applied in HF converter, no matter it is under soft or hard switching. To verify fast response of proposed VCC, the term of relative measurement error ($\varepsilon_r = \frac{|R_{DSon(R.)}(t) - \overline{R_{DSon(R.)}}|}{\overline{R_{DSon(R.)}}}$) is used. Its average value ($\overline{\varepsilon_r}$) of different time intervals (10–100 ns, 100 ns–1 μs and after 1 μs) are then compared in Fig. 7(c). $\overline{\varepsilon_r}$ is inferior to 1.6% when t_{on} is longer than 10 ns, which confirms fast dynamic response of proposed VCC to obtain DUT R_{DSon} when DUT switches in megahertz range power converter. The proposed circuit is validated in this section and a control

signal of TZCM will be presented in the next section to improve measurement sensitivity when device switches in HF converter.

III. MEASURING GaN DEVICE DYNAMIC R_{DSon} IN HF CONVERTER

The conventional device characterization method based on TCM is used to measure GaN device dynamic R_{DSon} when device operates in HF converter [17], [21]. Measurement error caused by unavoidable circuit parasitic inductance L_c under TCM on device ON-state resistance has been raised by authors in [21]. However, there is no solution proposed to compensate the measurement error. In this section, different sensitivity issues caused by unavoidable L_c and measurement probes deskew are studied. In order to improve measurement sensitivity when device is operated in HF power converter, a TZCM is proposed accordingly.

A. Triangle Current Mode

Under I_D current fast transition of TCM, the influence of unavoidable L_c [see Fig. 2(b)] due to PCB tracks, device packaging etc., deskew (t_{dk}) between voltage probe and current probe, and oscilloscope offset voltage accuracy (V_{off}, due to internal offset voltage source precision [22]) on dynamic R_{DSon} measurement sensitivity needs to be carefully studied when DUT is operated in HF converter.

Real DUT R_{DSon} is defined by

$$R_{\mathrm{DSon}}(t) = \frac{V_{\mathrm{DSon}}(t)}{I_D(t)}. \tag{1}$$

By considering the presence of L_c and oscilloscope offset V_{off}, measured apparent voltage $V_{\mathrm{DSon(m.)}}$ is

$$V_{\mathrm{DSon(m.)}}(t) = I_D(t) \cdot R_{\mathrm{DSon}}(t) + L_c \frac{dI_D(t)}{dt} + V_{\mathrm{off}}. \tag{2}$$

By considering t_{dk} between current probe and voltage probe, relation between measured apparent current $I_{D(m.)}(t)$ and real current $I_D(t)$ can then be further expressed by

$$I_{D(m.)}(t) = I_D(t) - t_{\mathrm{dk}} \cdot \frac{dI_D(t)}{dt}. \tag{3}$$

By combining (2) and (3), relative measurement error is therefore obtained by

$$\varepsilon_r = \frac{R_{\mathrm{DSon(m.)}}(t) - R_{\mathrm{DSon}}(t)}{R_{\mathrm{DSon}}(t)} = f\left(L_c, t_{\mathrm{dk}}, V_{\mathrm{off}}\right)$$

$$= \frac{t_{\mathrm{dk}}}{I_{D(m.)}(t)} \cdot \frac{dI_D(t)}{dt} + \frac{L_c}{R_{\mathrm{DSon}}(t) \cdot I_{D(m.)}(t)} \cdot \frac{dI_D(t)}{dt}$$

$$+ \frac{V_{\mathrm{off}}}{R_{\mathrm{DSon}}(t) \cdot I_{D(m.)}(t)}. \tag{4}$$

Supposing a symmetrical TCM is applied with $D = 50\%$ and $I_{D(m.)}(t)$ is measured at its maximal value, following term $\frac{1}{I_{D(m.)}(t)} \cdot \frac{dI_D(t)}{dt}$ can be simplified into $4f_{\mathrm{sw}}$, which is only dependent on DUT switching frequency f_{sw}. The influence of each variable L_c, t_{dk}, and V_{off} on ε_r is obtained by partial derivative of the function $f(L_c, t_{\mathrm{dk}}, V_{\mathrm{off}})$. They are then compared by the following:

$$g_{t_{\mathrm{dk}}} = \frac{\partial f\left(t_{\mathrm{dk}}, L_c, V_{\mathrm{off}}\right)}{\partial t_{\mathrm{dk}}} = 4f_{\mathrm{sw}}$$

$$g_{L_c} = \frac{\partial f\left(t_{\mathrm{dk}}, L_c, V_{\mathrm{off}}\right)}{\partial L_c} = \frac{4f_{\mathrm{sw}}}{R_{\mathrm{DSon}}(t)}$$

$$g_{V_{\mathrm{off}}} = \frac{\partial f\left(t_{\mathrm{dk}}, L_c, V_{\mathrm{off}}\right)}{\partial V_{\mathrm{off}}} = \frac{1}{R_{\mathrm{DSon}}(t) \cdot I_{D(m.)}(t)}. \tag{5}$$

Supposing DUT switches at 1 MHz, measured $I_{D(m.)}(t)$ is about 2 A and $R_{\mathrm{DSon}}(t)$ is about 0.2 Ω (same condition as results presented in Section II-B). The influence of each term on measurement error is obtained below.

1) $g_{t_{\mathrm{dk}}}$: The influence of t_{dk} on measurement error shows directly proportional dependence on DUT switching frequency. When $f_{\mathrm{sw}} = 1$MHz, $g_{t_{\mathrm{dk}}} = 0.004/\mathrm{n}s$, which means 1 ns of uncorrected deskew between voltage and current probes results in 0.4% measurement error. Even though different probes deskew detecting methods have been analyzed in [23], it still needs special caution to accurately obtain this value.

2) g_{L_c}: The influence of L_c on measurement error shows directly proportional dependence on DUT switching frequency and inversely proportional dependence on DUT R_{DSon} value. For the characterized DUT as an example, $g_{L_c} = 0.02/\mathrm{n}H$, which means 1 nH of unknown L_c value results in 2% measurement error. It is to be noted that part of L_c is from DUT packaging, which is not always an obvious parameter for power electronics engineers.

3) $g_{V_{\mathrm{OFF}}}$: The influence of V_{OFF} on measurement error shows inversely proportional dependence on DUT R_{DSon} value and switching current. In the chosen example, $g_{V_{\mathrm{OFF}}} = 0.0025/\mathrm{m}V$, which means 1 mV of oscilloscope offset voltage error results in 0.25% measurement error. It is to be noted that unlike $g_{t_{\mathrm{dk}}}$ and g_{L_c}, $g_{V_{\mathrm{off}}}$ is not dependent on f_{sw} and it is only determined by oscilloscope vertical voltage range setting, of which the value can be easily calibrated.

In the experimental work of this article, measurement oscilloscope is 8 b with 1-GHz bandwidth (DPO4104B). A Hall effect current probe (100 MHz, 1 A/V) is used to measure I_L and a passive voltage probe (500 MHz) is used to measure $V_{\mathrm{DS(m.)}}$. t_{dk} of chosen probes is around 10 ns, L_c is estimated to be 10 nH and V_{off} is within 1.5% of full voltage range (5 V with 500 mV/div). Therefore, each measurement error is: $g_{t_{\mathrm{dk}}} = 4\%$, $g_{L_c} = 20\%$, and $g_{V_{\mathrm{off}}} = 19\%$. It is to be noted that DUT can be placed at the same board with DSC and VCC to reduce L_c. However, it is not convenient in this design to characterize different devices.

Thus, total measurement error by applying the error propagation is

$$g_{\mathrm{total}} = \sqrt{g_{t_{\mathrm{dk}}}^2 + g_{L_c}^2 + g_{V_{\mathrm{off}}}^2} \approx 28\%. \tag{6}$$

It is shown from the above analysis that special caution is necessary to measure DUT R_{DSon} under TCM, which requires additional knowledge to accurately obtain t_{dk} and L_c and exclude their influence on obtained R_{DSon}. In order to improve measurement accuracy, it is proposed in the next section to measure DUT R_{DSon} under TZCM.
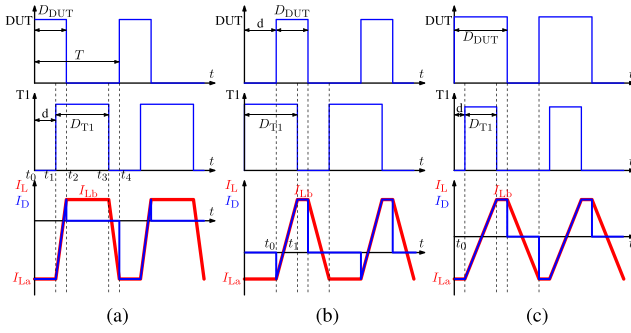
Fig. 8. Three current submodes of TZCM. (a) Submode 1. (b) Submode 2. (c) Submode 3.
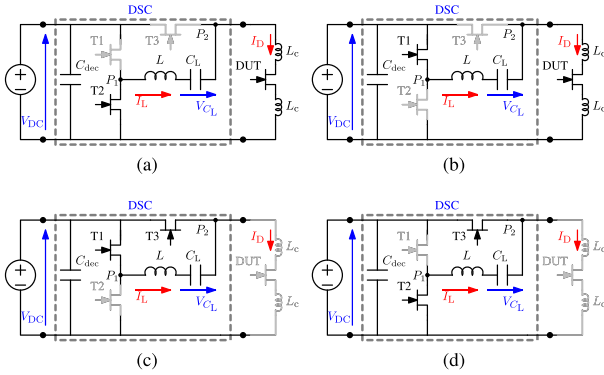

Fig. 9. Different circuit operation stages under submode 1 of TZCM. (a) From $t_0 - t_1$. (b) From $t_1 - t_2$. (c) From $t_2 - t_3$. (d) From $t_3 - t_4$.

B. Trapezoidal Current Mode

Unlike TCM, where DUT and T1 share the same control signal, control signal of T1 is different from DUT in TZCM. As DSC is a standard H-bridge, a phase shift d is applied between two legs. Ignoring effect of parasitic inductance L_c, when circuit is operated under TZCM, it should be ensured that there is no voltage across L when both legs are in the same switching state ("DUT ON, T1 OFF" and "DUT OFF, T1 ON"). Since these states correspond to nodes P_1 and P_2 having the same potential, this implies that there is no net voltage across capacitor C_L ($V_{C_L} = 0$). Consequently, both legs must be controlled with the same duty cycle: $D_{T1} = D_{T3}$, which means $D_{T1} + D_{DUT} = 1$. When the two legs are in different switching states, V_{dc} is applied across L with phase shift controlling the amplitude of I_L trapezoidal waveform. Depending on DUT duty cycle (D_{DUT}), there are three current submodes in TZCM method, which is illustrated in Fig. 8. T2 and T3 are still complementary control signals of T1 and DUT, respectively, with a deadtime τ. As τ is much smaller than switching period, it is neglected in the analysis.

1) Submode 1: From $t_0 - t_1$ [see Fig. 9(a)]: DUT is turned ON by negative load current I_{La} at t_0 in ZVS. As T1 is delayed to DUT control signal by d, DUT is in reverse conduction by an almost constant I_{La} during the delay time. Therefore, DUT $R_{DSon(R.)}$ can be measured under I_{La}. From $t_1 - t_2$ [see Fig. 9(b)]: both DUT and T1 are in ON-state, therefore I_L is charged by V_{dc} at this stage. From $t_2 - t_3$ [see Fig. 9(c)]: both T1 and T3 are in ON-state, I_L is with almost constant value I_{Lb}. From $t_3 -$

t_4 [see Fig. 9(d)]: both T2 and T3 are in ON-state, I_L is thus reversely charged by V_{dc}. Therefore, following two equations are applied:

$$V_{dc} = L \cdot \frac{(I_{Lb} - I_{La}) \cdot f_{sw}}{D_{DUT} - d}$$
$$\times I_{La} \cdot d + I_{Lb} \cdot (D_{T1} - (D_{DUT} - d))$$
$$+ (I_{La} + I_{Lb}) \cdot (D_{DUT} - d) = 0. \qquad (7)$$

By simplifying (7), I_{La} can be expressed by

$$I_{La} = -\frac{V_{dc} \cdot (D_{DUT} - d)}{f_{sw} \cdot L} \cdot D_{T1}. \qquad (8)$$

2) Submode 2: Control signal of DUT is delayed to T1 by d, so DUT is turned ON by negative load current I_{La} at t_0 in ZVS. As both T1 and DUT remain ON-state afterward, I_L is charged by V_{dc} to alternate direction. When T1 is turned OFFat t_1, DUT is in forward conduction by an almost constant I_{Lb} until it is turned OFF. Therefore, DUT $R_{DSon(F.)}$ can be measured under I_{Lb}. Following two equations are applied:

$$V_{dc} = L \cdot \frac{(I_{Lb} - I_{La}) \cdot f_{sw}}{D_{T1} - d}$$
$$\times I_{La} \cdot d + I_{Lb} \cdot (D_{DUT} - (D_{T1} - d))$$
$$+ (I_{La} + I_{Lb}) \cdot (D_{T1} - d) = 0. \qquad (9)$$

I_{Lb} can then be expressed by:

$$I_{Lb} = \frac{V_{dc} \cdot (D_{T1} - d)}{f_{sw} \cdot L} \cdot D_{T1}. \qquad (10)$$

3) Submode 3: DUT is turned on by negative load current I_{La} at t_0 in ZVS. Similar as submode 1, DUT $R_{DSon(R.)}$ can be measured under an almost constant I_{La} until T1 is turned ON. I_L is charged by V_{dc} to alternate direction during T1 ON-state. Afterward, similar to submode 2, DUT $R_{DSon(F.)}$ can be measured under an almost constant I_{Lb}. Following two equations are applied:

$$V_{dc} = L \cdot \frac{(I_{Lb} - I_{La}) \cdot f_{sw}}{D_{T1}}$$
$$\times I_{La} \cdot d + I_{Lb} \cdot (D_{DUT} - (D_{T1} + d))$$
$$+ (I_{La} + I_{Lb}) \cdot D_{T1} = 0. \qquad (11)$$

I_{La} and I_{Lb} can then be expressed by

$$I_{La} = -\frac{V_{dc} \cdot (D_{DUT} - d)}{f_{sw} \cdot L} \cdot D_{T1}$$
$$I_{Lb} = \frac{V_{dc} \cdot (D_{T1} + d)}{f_{sw} \cdot L} \cdot D_{T1}. \qquad (12)$$

By adding one degree of liberty d in TZCM, $R_{DSon(R.)}$ and $R_{DSon(F.)}$ can be measured under same I_{La} and I_{Lb} value with a constant L value in different f_{sw} and D_{DUT}, which is not the case by TCM method, where L value needs to be changed with f_{sw} and D_{DUT} to keep load current constant.

It is to be noted that for safety reason, it is preferred to add an external capacitor C_L in the circuit to withstand any unbalanced average voltage between P_1 and P_2 to be applied to L, which may
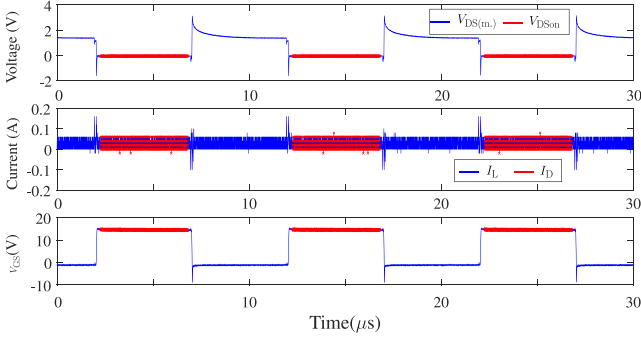
Fig. 10. Obtained device $V_{\rm DS(m.)}$, $I_{\rm D}$ and $V_{\rm GS}$ waveform to calibrate oscilloscope $V_{\rm off}$.

TABLE IV
$V_{\rm off}$ CALIBRATED RESULTS ON BOTH VOLTAGE AND CURRENT MEASUREMENT

	μ (mV)	σ (mV)	$V_{\rm FS}$ (V)	$\frac{\mu}{V_{\rm FS}}$
$V_{\rm off}(V)$	-59	3	5 (0.5V/div.)	1.2%
$V_{\rm off}(I)$	27	0.6	5 (0.5V/div.)	0.5%

result in infinite increase of $I_{\rm L}$. Unbalanced average voltage may be caused by inhomogeneous delays in the gate driver of each transistor (it may slightly influence on $D_{\rm DUT}$ and $D_{\rm T1}$), ON-state voltage drops of the transistors and deadtime of two transistors of each bridge (it may slightly influence on each stage length). The resulting $V_{C_{\rm L}}$ value can be neglected in all the experimental results, so $I_{\rm L}$ is still under trapezoidal waveform, which can be proved by measurement results presented in Section IV of the article.

It can be also concluded that unlike TCM method, DUT $R_{\rm DSon}$ is measured at constant load current, which simultaneously resolves two of the measurement sensitivity issues highlighted in Section III-A regarding the influence of measurement probe $t_{\rm dk}$ and of parasitic circuit and package inductance L_c on measurement results. Only $V_{\rm off}$ needs to be predetermined for accurate measurement, which will be presented in the next section.

C. $V_{\rm off}$ Calibration

In order to calibrate oscilloscope offset voltage $V_{\rm off}$, L and $C_{\rm L}$ are disconnected from the measurement circuit in Fig. 2(b). When DUT (SiC-MOSFET) switches at 100 kHz and $V_{\rm dc} = 200$ V, obtained device $V_{\rm DS(m.)}$, $I_{\rm D}$ and $V_{\rm GS}$ is shown in Fig. 10.

When $V_{\rm GS}$ equals to 16 V, DUT is in ON-state. As there is no current flowing through DUT, both of measured $I_{\rm D}$ and $V_{\rm DSon}$ should be zero. The above measurement process is repeated 20 times by connecting and disconnecting voltage and current probes. Therefore, $V_{\rm off}$ mean value (μ) and standard derivation (σ) on both voltage ($V_{\rm off}(V)$) and current ($V_{\rm off}(I)$) measurement are obtained and they are compared with each oscilloscope channel full range value ($V_{\rm FS}$) in Table IV.

It can be concluded that obtained $V_{\rm off}$ is consistent by a small σ value. Meanwhile, obtained $\frac{\mu}{V_{\rm FS}}$ shows relative voltage offset error to channel full range voltage, which might be different in
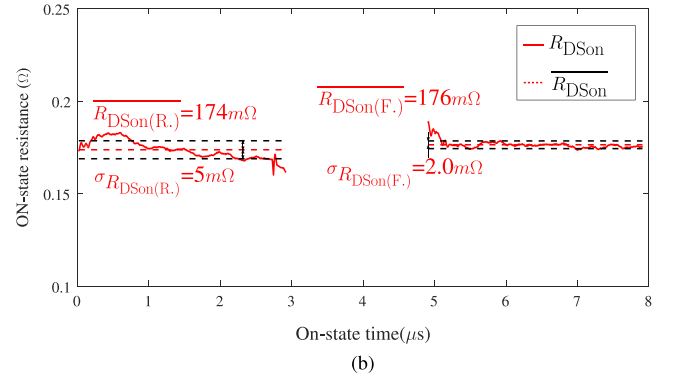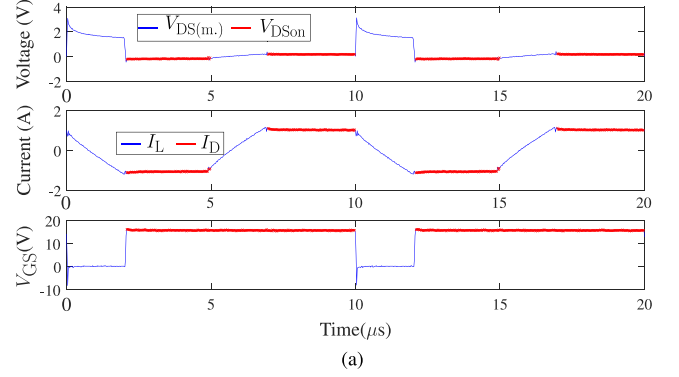

Fig. 11. SiC-MOSFET reverse and forward ON-state resistance measurement results when device switches at 100 kHz by proposed TZCM. (a) Measured waveforms. (b) $R_{\rm DSon(R.)}$ and $R_{\rm DSon(F.)}$ of one switching period.

different manufacturers. After compensation, σ remains an unpredictable error source. However, its influence on measurement results is less than 1% ($g_{V_{\rm off}} \times \sigma = 0.75\%$).

After calibrating $V_{\rm off}$, $R_{\rm DSon}$ of both SiC-MOSFET and GaN-HEMT are obtained when they operate continuously in power converter.

IV. MEASUREMENT RESULTS

A. SiC-MOSFET

In order to validate the proposed TZCM method, $R_{\rm DSon}$ of the same SiC-MOSFET is measured when device is switching at 100 kHz ($D_{\rm DUT} = 80\%$), $V_{\rm dc} = 200$ V to compare with its values obtained in Fig. 7(c). Obtained device $V_{\rm DS(m.)}$, $I_{\rm L}$ and $V_{\rm GS}$ waveform are shown in Fig. 11(a) under submode 3 of TZCM. When $V_{\rm GS} = 16$ V, $V_{\rm DSon}$ and $I_{\rm D}$ can be obtained from measured $V_{\rm DS(m.)}$ and $I_{\rm L}$ waveforms. Therefore, both $R_{\rm DSon(R.)}$ and $R_{\rm DSon(F.)}$ can be measured simultaneously at one switching period under constant current.

As compared in Fig. 11(b), obtained $\overline{R_{\rm DSon(R.)}}$ is about 174 mΩ, and its $\sigma_{R_{\rm DSon(R.)}}$ is about 5 mΩ, which is 2.9% to $\overline{R_{\rm DSon(R.)}}$ value. Obtained $\overline{R_{\rm DSon(F.)}}$ is about 176 mΩ, and its $\sigma_{R_{\rm DSon(F.)}}$ is about 2.0 mΩ, which is 1.1% to $\overline{R_{\rm DSon(F.)}}$ value. Both $\overline{R_{\rm DSon(R.)}}$ and $\overline{R_{\rm DSon(F.)}}$ are slightly increased (7.4% and 1.7%) in comparison with their values shown in Table III, which may be due to DUT junction temperature $T_{\rm j}$ difference when it is operated at 100 kHz. Measurement consistency and accuracy of the proposed measurement circuit and TZCM method can be verified by those results.
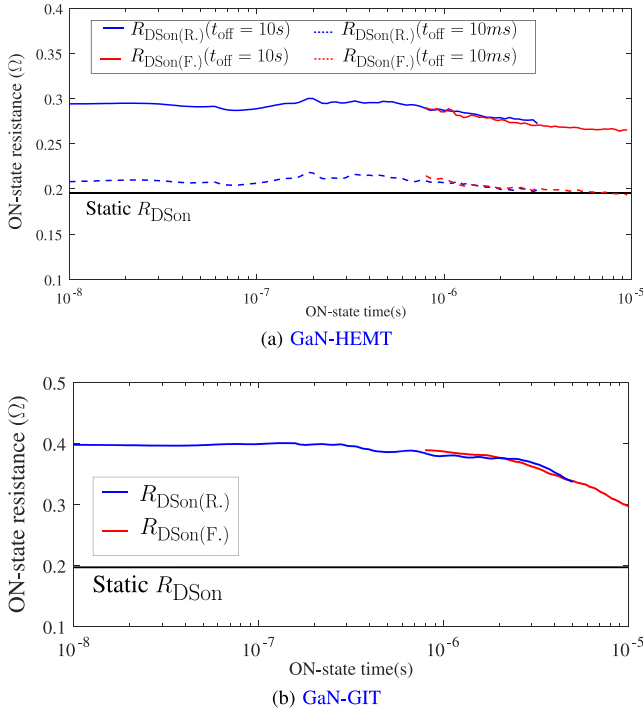
Fig. 12.   Reverse and forward dynamic R_{DSon} of different GaN transistors. (a) GaN-HEMT. (b) GaN-GIT.

B. GaN-HEMT

1) Single-Pulse Mode: In order to investigate GaN transistor $R_{\text{DSon(R.)}}$ and $R_{\text{DSon(F.)}}$ with t_{on}, its dynamic R_{DSon} under both reverse and forward conduction is measured at first under single-pulse mode by the same method presented in Section II-B.

A GaN-HEMT (GS66502B, 650 V/7.5 A, $V\text{th} = 1.3$ V) with similar static R_{DSon} of around 200 mΩ is characterized when t_{off} of Fig. 5 is set to be 10 ms and 10 s. As shown in Fig. 12(a), in comparison with device static R_{DSon} value (0.195 Ω), device dynamic R_{DSon} value can increase to 50% bigger and it increases more with longer t_{off}. It is also observed in the measurement results that obtained $R_{\text{DSon(F.)}}$ corresponds well to the $R_{\text{DSon(R.)}}$ value on the common t_{on} range (800 to 3 μs), which confirms that dynamic R_{DSon} value decreases to static R_{DSon} value with t_{on}. This result conforms to reported GaN device dynamic R_{DSon} variation in the literature [17] and can be used as a reference to verify measurement results when device is operated in HF switching converter. It is also shown in the results that GaN-HEMT does not have body-diode to lower its $R_{\text{DSon(R.)}}$ than $R_{\text{DSon(F.)}}$. Obtained device dynamic R_{DSon} under both reverse and forward conduction is due to trapped charge.

Another GaN gate injection transistor (GIT, PGA26E19BA, 600 V/13 A) has been tested with the same method under conditions: $V_{\text{DS}} = 200$ V, $I_{\text{D}} = 2$A, and $t_{\text{off}} = 10$ s. As presented in Fig. 12(b), it reveals again that obtained $R_{\text{DSon(R.)}}$ corresponds to $R_{\text{DSon(F.)}}$ value on the common t_{on} range, owing to the accuracy of proposed measurement circuit. For this GIT, dynamic R_{DSon} increases twice bigger than its static R_{DSon} value when t_{on} is less than 100 ns, revealing an nonnegligible effect on device conduction losses.
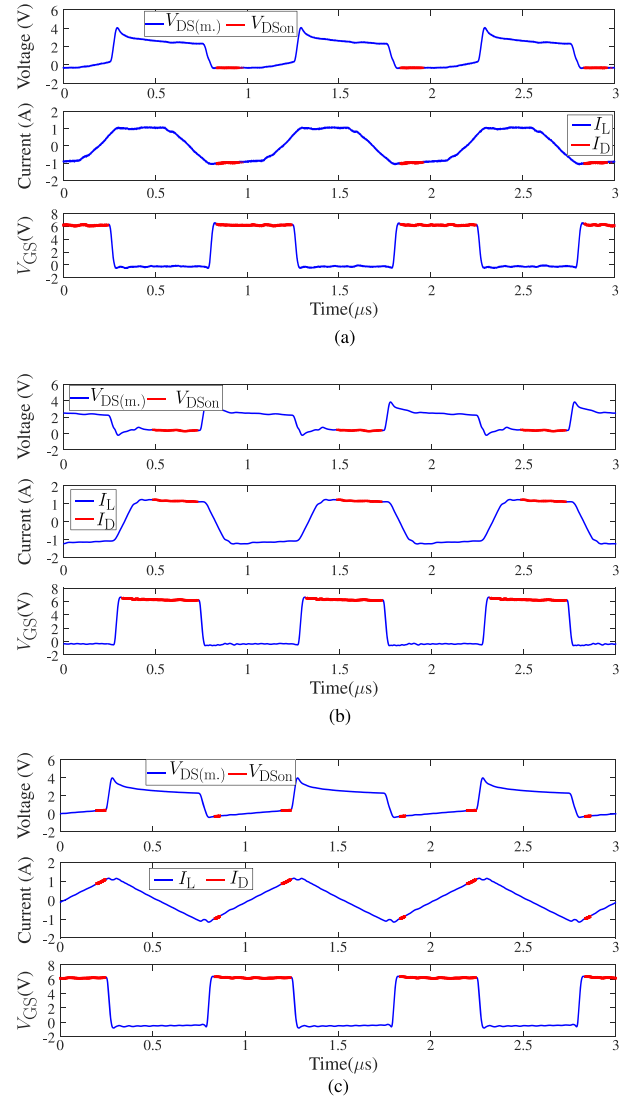

Fig. 13.   GaN-HEMT dynamic ON-state resistance measurement results by proposed TZCM and by conventional TCM when device switches at 1 MHz. (a) Device switches at submode 1 of TZCM. (b) Device switches at submode 2 of TZCM. (c) Device switches at TCM.

2) Continuous Mode: When device is switching at 1 MHz ($D_{\text{DUT}} = 50\%$) and $V_{\text{dc}} = 200$ V, dynamic R_{DSon} of the same GaN-HEMT is then measured by the proposed TZCM and conventional TCM method, where the measurement results are shown in Fig. 13. It can be noted that when DUT is fully turned ON at $V_{\text{GS}} = 6$ V, obtained V_{DSon} is negative in all the experimental results, which confirms that DUT is under reverse conduction and it realizes ZVS soft switching at turn-ON transition, as its C_{oss} is fully discharged by I_{L} during deadtime.

By using TZCM method, $R_{\text{DSon(R.)}}$ is obtained under constant reverse I_{D} at submode 1 [see Fig. 13(a)] and $R_{\text{DSon(F.)}}$ is obtained under constant forward I_{D} at submode 2 [see Fig. 13(b)]. By using conventional TCM method, device R_{DSon} is obtained when I_{D} is around 1 A in both reverse and forward conduction [see Fig. 13(c)]. Obtained R_{DSon} and their mean value $\overline{R_{\text{DSon}}}$ over the chosen conduction time by the two methods are then compared in Fig. 14. $\sigma_{R_{\text{DSon}}}$ is inferior to 3 mΩ in all the obtained data, which confirms again the measurement
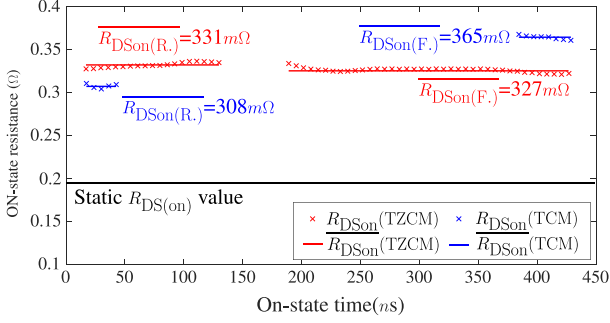
Fig. 14. GaN-HEMT dynamic ON-state resistance comparison between TZCM and TCM.

consistency by using the proposed circuit. Therefore, $\overline{R_{\mathrm{DSon}}}$ can be used to compare the measurement accuracy of different methods.

By conventional TCM method, obtained GaN-HEMT dynamic $\overline{R_{\mathrm{DSon(R.)}}}$ is 308 mΩ and $\overline{R_{\mathrm{DSon(F.)}}}$ is 365 mΩ. The difference ($\Delta R = \overline{R_{\mathrm{DSon(R.)}}} - \overline{R_{\mathrm{DSon(F.)}}}$) is -56 mΩ, which is about -18.5% to $\overline{R_{\mathrm{DSon(R.)}}}$ value. The increase of device dynamic ON-state resistance value during one switching period with ON-state time does not agree with GaN device physics shown in Fig. 12(a). As shown in Section III-A, influence of t_{dk} and L_c on measurement sensitivity becomes critical under fast I_L transition [more than 5 A/μs as shown in Fig. 13(c)]. This negative ON-state resistance difference can be further explained by (2), where the term $\frac{\mathrm{d}I_D}{\mathrm{d}t}$ lowers apparent $V_{\mathrm{DSon(m.)}}$ value when DUT is in reverse conduction and increases $V_{\mathrm{DSon(m.)}}$ value when DUT is in forward conduction.

In comparison, by proposed TZCM, obtained GaN-HEMT $\overline{R_{\mathrm{DSon(R.)}}}$ is 331 mΩ and $\overline{R_{\mathrm{DSon(F.)}}}$ is 327 mΩ at one period. ΔR is only 4 mΩ, which is about 1.2% to $\overline{R_{\mathrm{DSon(R.)}}}$ value. This slight decrease of device dynamic R_{DSon} with ON-state time at one switching period conforms to obtained GaN device dynamic ON-state resistance values in Fig. 12(a), which also demonstrates the advantage of proposed TZCM method over conventional TCM method on measurement accuracy when circuit L_c cannot be ignored in HF power converter. It is to be noted that L_c can be reduced by using an all-integration PCB board. Nevertheless, as presented in (5), designers would still have unavoidable g_{L_c} measurement issue depending on device switching frequency and R_{DSon} value by using conventional TCM method.

V. CONCLUSION

In this article, a measurement circuit is proposed to measure GaN transistor dynamic ON-state resistance R_{DSon} when device is operated in HF converters. The measurement circuit is constituted by a standard H-bridge to control DSC and a VCC to reduce measured voltage from full dc-bus voltage to a few volts, so as to improve measurement resolution. In comparison with different state-of-the-art of VCC, the proposed one has a simple structure (only three components), good dynamic response (10 ns) and can be used to measure power transistor both reverse and forward R_{DSon} with robust accuracy, which is suitable for device application in soft switching circuit. The measurement circuit is then validated by measuring on SiC-MOSFET with constant R_{DSon} value when device is under both reverse and forward conduction.

Afterward, influence of unavoidable common parasitic inductance L_c between DSC and VCC, voltage and current probes deskew (t_{dk}) and oscilloscope offset voltage (V_{off}) on measurement sensitivity is analyzed, which shows potential sensitivity issue in conventional device R_{DSon} measurement by TCM method when device operates in HF converter. In order to eliminate the influence of L_c and t_{dk} on measurement sensitivity, a TZCM method is proposed. By adding a phase shift between two phases of a H-bridge, transistor R_{DSon} can be obtained under an almost constant drain current. Therefore, only V_{off} needs to be calibrated in TZCM method, in which its value can be easily obtained by a measurement when DUT operates without current.

Reverse and forward ON-state resistances ($R_{\mathrm{DSon(R.)}}$ and $R_{\mathrm{DSon(F.)}}$) of the same SiC-MOSFET are measured by TZCM when device operates at 100 kHz. Measurement results conform to their values obtained by a curve tracer, which validates consistency and accuracy of proposed TZCM method. Following that, when device switches at 1 MHz, GaN device dynamic R_{DSon} is measured by both TZCM method and conventional TCM method. It is shown in the measurement results, the sensitivity issue caused by t_{dk} and L_c in conventional TCM method under fast transition of drain current, which causes a nonphysical device dynamic R_{DSon} increase with ON-state time. The advantage of proposed TZCM method on measurement accuracy is thus justified.

Based on the results of the article, a GaN device model taking into consideration of device dynamic R_{DSon} evaluation under different operation conditions can be built and validated, which will be the subject of future communications.

REFERENCES

[1] W. Zhang, F. Wang, D. J. Costinett, L. M. Tolbert, and B. J. Blalock, "Investigation of gallium nitride devices in high-frequency LLC resonant converters," *IEEE Trans. Power Electron.*, vol. 32, no. 1, pp. 571–583, Jan. 2017.

[2] M. Guz *et al.*, "IEEE ITRW working group position paper-system integration and application: Gallium nitride: Identifying and addressing challenges to realize the full potential of GaN in power conversion applications," *IEEE Power Electron. Mag.*, vol. 5, no. 2, pp. 34–39, Jun. 2018.

[3] S. Jiang *et al.*, "All-GaN-integrated cascode heterojunction field effect transistors," *IEEE Trans. Power Electron.*, vol. 32, no 11, pp. 8743–8750, Nov. 2017.

[4] M. Fu, C. Fei, Y. Yang, Q. Li, and F. Lee, "Optimal design of planar magnetic components for a two-stage GaN-based dc/dc converter," *IEEE Trans. Power Electron.*, vol. 34, no. 4, pp. 3329–3338, Apr. 2019.

[5] M. S. Haque and S. Choi, "Prognosis of enhance mode gallium nitride high electron mobility transistors using on-state resistance as fault precursor," in *Proc. IEEE Energy Convers. Congr. Expo.*, Oct. 2017, pp. 1988–1994.

[6] M. A. Eleffendi and C. M. Johnson, "In-service diagnostics for wire-bond lift-off and solder fatigue of power semiconductor packages," *IEEE Trans. Power Electron.*, vol. 32, no. 9, pp. 7187–7198, Sep. 2017.

[7] W. Saito *et al.*, "Field-plate structure dependence of current collapse phenomena in high-voltage GaN-HEMTs," *IEEE Electron Device Lett.*, vol. 31, no. 7, pp. 659–661, Jul. 2010.

[8] M. Uren and M. Kuball, "GaN transistor reliability and instabilities," in *Proc. 10th Int. Conf. Adv. Semicond. Devices Microsyst.*, Oct. 2014, pp. 1–8.

[9] H. Chandrasekar *et al.*, "Buffer-induced current collapse in GaN HEMTs on highly resistive Si substrates," *IEEE Electron Device Lett.*, vol. 39, no. 10, pp. 1556–1559, Oct. 2018.

[10] B. J. Galapon, A. J. Hanson, and D. J. Perreault, "Measuring dynamic on resistance in GaN transistors at MHz frequencies," in *Proc. IEEE 19th Workshop Control Model. Power Electron.*, Jun. 2018, pp. 1–8.

[11] N. Badawi, O. Hilt, E. Bahat-Treidel, J. Böcker, J. Würfl, and S. Dieckerhoff, "Investigation of the dynamic on-state resistance of 600V normally-off and normally-on GaN HEMTs," *IEEE Trans. Ind. Appl.*, vol. 52, no. 6, pp. 4955–4964, Nov./Dec. 2016.

[12] Y. Cai, A. J. Forsyth, and R. Todd, "Impact of GaN HEMT dynamic on-state resistance on converter performance," in *Proc. IEEE Appl. Power Electron. Conf. Expo.*, Mar. 2017, pp. 1689–1694.

[13] F. Yang, C. Xu, and B. Akin, "Quantitative analysis of different operating conditions' effect on dynamic on-resistance in enhancement-mode GaN HEMTs," in *Proc. IEEE 6th Workshop Wide Bandgap Power Devices Appl.*, Oct. 2018, pp. 134–140.

[14] T. Foulkes, T. Modeer, and R. C. N. Pilawa-Podgurski, "Developing a standardized method for measuring and quantifying dynamic on-state resistance via a survey of low voltage GaN HEMTs," in *Proc. IEEE Appl. Power Electron. Conf. Expo.*, Mar. 2018, pp. 2717–2724.

[15] K. Li, P. L. Evans, and C. M. Johnson, "Characterisation and modeling of Gallium Nitride power semiconductor devices dynamic on-state resistance," *IEEE Trans. Power Electron.*, vol. 33, no. 6, pp. 5262–5273, Jun. 2018.

[16] B. Lu, T. Palacios, D. Risbud, S. Bahl, and D. Anderson, "Extraction of dynamic on-resistance in GaN transistors: Under soft- and hard-switching conditions," in *Proc. IEEE Comp. Semicond. Integr. Circuit Symp.*, Oct. 2011, pp. 1–4.

[17] R. Li, X. Wu, S. Yang, and K. Sheng, "Dynamic on-state resistance test and evaluation of GaN power devices under hard- and soft-switching conditions by double and multiple pulses," *IEEE Trans. Power Electron.*, vol. 34, no. 2, pp. 1044–1053, Feb. 2019.

[18] D. Han and B. Sarlioglu, "Deadtime effect on GaN-based synchronous boost converter and analytical model for optimal deadtime selection," *IEEE Trans. Power Electron.*, vol. 31, no. 1, pp. 601–612, Jan. 2016.

[19] R. Gelagaev, P. Jacqmaer, and J. Driesen, "A fast voltage clamp circuit for the accurate measurement of the dynamic on-resistance of power transistors," *IEEE Trans. Ind. Electron.*, vol. 62, no. 2, pp. 1241–1250, Feb. 2015.

[20] K. Li, P. Evans, and M. Johnson, "SiC/GaN power semiconductor devices: A theoretical comparison and experimental evaluation under different switching conditions," *IET Elect. Syst. Transp.*, vol. 8, no. 1, pp. 3–11, Mar. 2018.

[21] M. Guacci, D. Bortis, and J. W. Kolar, "On-state voltage measurement of fast switching power semiconductors," *CPSS Trans. Power Electron. Appl.*, vol. 3, pp. 163–176, Jun. 2018.

[22] *Understanding Key High-Performance Oscilloscope Specifications*, Tektronix, Beaverton, OR, USA, 2002.

[23] Z. Zhang, B. Guo, F. F. Wang, E. A. Jones, L. M. Tolbert, and B. J. Blalock, "Methodology for wide band-gap device dynamic characterization," *IEEE Trans. Power Electron.*, vol. 32, no. 12, pp. 9307–9318, Dec. 2017.
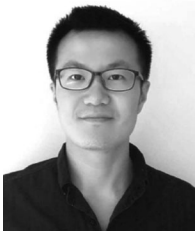
Ke Li (Member, IEEE) received the B.Eng. and M.Eng. degrees in electrical engineering from the Southwest Jiaotong University, Chengdu, China, in 2008 and 2011, respectively, the Eng. degree from Ecole Centrale de Marseille, Marseille, France, in 2011, and the Ph.D. degree in electrical engineering from the University of Lille, Lille, France, in 2014.

From 2015 to 2019, he was a Research Fellow with the University of Nottingham, Nottingham, U.K. In 2019, he was appointed as an Assistant Professor in power electronics, machines, and drives with Coventry University, Coventry, U.K. His research interests include wide-bandgap (SiC/GaN) power semiconductor devices integration to high power-density power converters, power converters electrothermal and electromagnetic modeling, and power converters electromagnetic interference mitigation.

Arnaud Videt (Member, IEEE) received the Ph.D. degree in electrical engineering from Ecole Centrale de Lille, Villeneuve-d'Ascq, France, in 2008.

He joined Schneider Toshiba Inverter, Pacy-sur-Eure, France, where his research focused on motor drive converter topologies and modulation strategies. Since 2010, he is an Associate Professor with the L2EP laboratory, University of Lille, Lille, France. His current research interests include wide-bandgap power devices and electromagnetic compatibility issues in power converters.

Nadir Idir (Member, IEEE) received the Ph.D. degree in electrical engineering from the University of Lille 1, Lille, France, in 1993.

He is a Full Professor with IUT A of the University of Lille 1, where he teaches power electronics and electromagnetic compatibility. Since 1993, he has been with the Laboratory of Electrical Engineering and Power Electronics (L2EP) of the University of Lille 1. His research interests include, design methodologies for HF switching converters, power devices (SiC and GaN), electromagnetic interference (EMI) in static converters, HF modeling of the passive components, EMI filter design methodologies for power converters.

Paul Leonard Evans received the M.Eng. degree in electrical and electronic engineering, and the Ph.D. degree in electrical engineering from the University of Nottingham, Nottingham, U.K., in 2007, and 2011, respectively.

In 2010, he became a Research Fellow with the University of Nottingham, where he was appointed as an Assistant Professor in 2013, and an Associate Professor in 2019. He currently leads the Virtual Prototyping work in the EPSRC Centre for Power Electronics, Nottingham, U.K. His expertise lies in the application of accelerated computational modeling techniques to the simulation of power electronic systems.

Dr. Evans' work on extraction of compact thermal models was awarded the IEEE Transactions on Power Electronics Second Prize Paper Award in 2013.

Christopher Mark Johnson (Member, IEEE) received the B.A. degree in engineering and the Ph.D. degree in electrical engineering from the University of Cambridge, Cambridge, U.K., in 1986 and 1991, respectively.

From 1990 to 1992, he was a Research Associate with the University of Cambridge, and in 1992, he was appointed as a Lecturer with Newcastle University, Newcastle upon Tyne, U.K., where his research included the design, analysis and characterization of power semiconductor devices, resonant power conversion, and instrumentation. From 1998 to 2001, he managed the U.K. National Programme on Silicon Carbide electronics, and in 2000, he became a Reader of power electronics with Newcastle University. In 2003, he was appointed as Rolls-Royce/RAEng Research Professor of Power Electronic Systems with the University of Sheffield, Sheffield, U.K. In 2006, he was appointed as a Personal Chair with the University of Nottingham, Nottingham, U.K., where he currently leads research into power semiconductor devices, power device packaging, reliability, thermal management, power module technologies and power electronic applications. He is the Director of the U.K. Engineering and Physical Sciences Research Council (EPSRC) Centre for Power Electronics, which combines the U.K.'s best academic talent to address the key research challenges underpinning power electronics, and is also a Leader of the Advanced Propulsion Centre (APC) Thematic Spoke in Power Electronics.